Author Manuscript

Author Manuscript

Author Manuscript

Author Manuscript

HHS Public Access

Author manuscript

Mech Dev. Author manuscript; available in PMC 2016 May 16.

Published in final edited form as:

Mech Dev. 2015 May ; 136: 123–132. doi:10.1016/j.mod.2014.12.005.

Fibulin-1 suppresses endothelial to mesenchymal transition in the proximal outflow tract

Keerthi Harikrishnan[a], **Marion A. Cooley**[a], **Yukiko Sugi**[a], **Jeremy L. Barth**[a], **Lars M. Rasmussen**[b], **Christine B. Kern**[a], **Kelley M. Argraves**[a,*], and **W. Scott Argraves**[a]

[a] Department of Regenerative Medicine and Cell Biology, Medical University of South Carolina, Charleston, SC 29425, USA

[b] Department of Clinical Biochemistry and Pharmacology, Odense University Hospital, Odense, Denmark

Abstract

Endothelial to mesenchymal transition (EMT) that occurs during cardiac outflow tract (OFT) development is critical for formation of the semilunar valves. Fibulin-1 (Fbln1) is an extra-cellular matrix protein that is present at several sites of EMT, including the OFT (i.e., E9.5–10.5). The aim of this study was to determine the role of Fbln1 in EMT during the earliest events of OFT development. Examination of proximal OFT cushions in Fbln1 null embryos detected hypercellularity at both E9.5 (93% increase; $p = 0.002$) and E10.5 (43% increase; $p = 0.01$) as compared to wild type, suggesting that Fbln1 normally suppresses OFT endocardial cushion EMT. This was supported by studies of proximal OFT cushion explants, which showed that explants from Fbln1 null embryos displayed a 58% increase in cells migrating from the explants as compared to wild type ($p = 0.005$). We next evaluated the effects of Fbln1 deficiency on the expression of factors that regulate proximal OFT EMT. At E9.5, Fbln1 null proximal OFT endocardium and EMT-derived mesenchyme showed increased TGFβ2 (58% increase; $p = 0.01$) and increased Snail1-positive nuclei (27% increase; $p = 0.0003$). Histological examination of OFT cushions in Fbln1 null embryos (E9.5) also detected cells present in the cushion that were determined to be erythrocytes based on round morphology, autofluorescence, and positive staining for hemoglobin. Erythrocytes were also detected in Fbln1 null OFT cushions at E10.5. Together, the findings indicate that Fbln1 normally suppresses proximal OFT EMT preventing proximal cushion hypercellularity and blood cell accumulation.

Keywords

Extracellular matrix; Fibulin-1; EMT; Proximal outflow tract; Endocardial barrier; Endocardial cushions; endothelial barrier

[*] Corresponding author. Department of Regenerative Medicine and Cell Biology, Medical University of South Carolina, Charleston, SC 29425, USA. Tel.: +1 843 792 3535; fax: +1 843 792 0664. argravek@musc.edu (K.M. Argraves)..

Appendix: Supplementary material

Supplementary data to this article can be found online at doi:10.1016/j.mod.2014.12.005.

Author Manuscript Author Manuscript Author Manuscript Author Manuscript

1. Introduction

Formation of the semilunar valves begins in the mouse between embryonic days (E) E8.5 and E9.0 when the primary myocardium secretes a hyaluronan-rich extracellular matrix (ECM) resulting in opposing swellings that form the proximal and distal OFT endocardial cushions (Butcher and Markwald, 2007). Subsequently, at approximately E10.5, a subset of endocardial cells within the proximal OFT undergo an endothelial to mesenchymal transformation (EMT) in response to region-specific myocardial and endocardial signals exchanged across this specialized ECM (Garside et al., 2012). The transformed endocardial cells invade this ECM until around E11.5 after which EMT ends (Combs and Yutzey, 2009). By E11.5, a second population of mesenchymal cells, the cardiac neural crest (NCC), infiltrate the distal OFT cushions to form the aorticopulmonary septum (Waldo et al., 1998). Fate mapping studies suggest that the neural crest and the EMT-derived cells remain as separate populations and that the interaction between these two population promotes the positioning and patterning of the semilunar valves within the OFT (Phillips et al., 2013; Wu et al., 2011). Ultimately, extensive growth and remodeling of the OFT cushions are required to form the final structured semilunar valve leaflets of the aorta and pulmonary artery (Barnett and Desgrosellier, 2003; Combs and Yutzey, 2009; Garside et al., 2012; Sizarov et al., 2012).

The essential role of the ECM in promoting proximal OFT EMT is evident in embryos deficient in hyaluronan synthase-2 (Has-2) (Camenisch et al., 2000) or versican, which die around E10.5 and display hypoplastic atrioventricular (AV) and OFT endocardial cushions (Mjaatvedt et al., 1998). Further analysis showed that hyaluronan (produced by Has-2) was required for ErbB receptor activation in order to induce EMT (Camenisch et al., 2002). Although soluble growth factors (Bai et al., 2013; Dor et al., 2001; Garside et al., 2012; Sakabe et al., 2012) involved in OFT endocardial cushion EMT have been extensively studied, our understanding of how ECM proteins present in the proximal cushion potentiate these signals is limited.

Fibulin-1 (Fbln1) is an ECM protein present in the OFT cushion of both chick (Bouchey et al., 1996) and mouse (Cooley et al., 2008) during cardiac development. Studies using chick cushion explants have showed that Fbln1 suppresses fibronectin-mediated cell migration (Twal et al., 2001), suggesting that Fbln1 may have an inhibitory role on cardiac cushion EMT.To evaluate the role of Fbln1 in proximal OFT EMT, we examined E9.5-E10.5 wild type and Fbln1 deficient embryos. Here we report a novel role for Fbln1 as a negative modulator of OFT EMT that represses TGFβ2 and Snail1 levels during cardiac semilunar valve morphogenesis.

2. Materials and methods

2.1. Fbln1 deficient mice

This study employed a *Fbln1* gene trap mutant that has previously been reported (Cooley et al., 2008). All animal procedures were approved by the MUSC Institutional Animal Care and Use Committee and complied with federal and institutional guidelines.

Author Manuscript Author Manuscript Author Manuscript Author Manuscript

2.2. Reagents used in immunohistochemistry

Primary antibodies used in this study were rabbit anti-Fbln1 (Argraves et al., 1990), mouse anti-α-smooth muscle actin (αSMA) (Sigma Chemical Corp, St. Louis, MO), mouse anti-transforming growth factor-β2 (Abcam, Cambridge, MA), goat anti-Snail1 (Abcam), rabbit anti-phospho-histone H3 (PHH3) (Millipore, Billerica, MA), and goat anti-VE-Cadherin (Santa Cruz Biotechnology, Dallas, TX). The primary antibodies were detected with the following secondary antibodies: Cy5-labeled donkey anti-rabbit IgG (Jackson Immunoresearch Laboratories), Cy5-labeled donkey anti-mouse IgG (Jackson Immunoresearch Laboratories), Alexa Fluor 568-labeled goat anti-rabbit IgG (Life Technologies, Carlsbad, CA), Alexa Fluor 488-labeled donkey anti-goat IgG (Life Technologies) and Alexa Fluor 488-labeled donkey anti-mouse IgG (Life Technologies).

2.3. Histology and immunohistochemistry

Wild type and Fbln1-deficient (E9.5–10.5) embryos were obtained from timed pregnant Fbln1 heterozygous matings. PCR was used to genotype embryonic tissue as described previously (Cooley et al., 2008). E9.5 and E10.5 wild type and Fbln1 embryos were fixed in 4% paraformaldehyde, PBS. For Fbln1 staining, tissue was embedded in Optimal Cutting Temperature (OCT) compound and sectioned at 10 m thickness. Anti-Fbln1 immunolabeling was performed on frozen tissue sections containing E9.5-E10.5 OFT regions from wild type and Fbln1 null embryos. For immunohistochemical detection of other proteins, fixed E9.5-E10.5 wild type and Fbln1 null embryos were embedded in paraffin, sectioned at 5 μm, and subjected to heat-induced antigen retrieval using a citric acid solution (H-3300, Vector Laboratories Burlingame, CA). Sections were treated with 1% BSA in PBS for 1 h followed by overnight incubation with primary antibodies for TGFβ2, Snail1, PHH3 or αSM actin. Bound primary antibodies were detected using fluorescently conjugated anti-mouse and anti-goat secondary antibodies. Nuclei were labeled with DRAQ5 (Cell Signaling, Danvers, MA) or Hoechst (Molecular Probes, Invitrogen Corp., Carlsbad, CA). Hematoxylin and eosin (H&E) staining was performed on paraffin sections using standard protocols. Fbln1 null OFT sections were used as negative controls for Fbln1 immunolabeling. Species-appropriate normal IgGs were used in place of primary antibodies as negative controls for TGFβ2 and Snail1 immunolabeling.

2.4. Proliferation and apoptosis assays

The percentage of PHH3 positive cells in proximal OFT (E9.5 and E10.5) was calculated by counting the number of anti-PHH3 positive cells relative to the total number of nuclei using the Adobe Photoshop Count tool. For apoptosis analysis, TdT-mediated dUTP Nick-End (TUNEL) assay was performed on paraffin sections (E10.5) using the Apo Tag system (Millipore) as per manufacturer's instructions.

2.5. Morphometric analysis

3D reconstructions of proximal OFT cushions (E9.5) were generated using AMIRA. The anatomical dogleg bend at E9.5 was used as a boundary between the distal and proximal OFT cushions (Anderson et al., 2003). ImageJ software (NIH) was used to perform area measurements. Volumetric measurements were calculated using the voxel size and the tissue

Author Manuscript Author Manuscript Author Manuscript Author Manuscript

thickness. Total cell counts (i.e., endothelial cells, mesenchymal and blood cells) were tabulated using the Adobe Photoshop counting tool. Endothelial cells were defined by positive staining for VE-Cadherin, which is a marker of endothelial cells. Erythrocytes were identified by Giemsa staining, distinct rounded morphology and/or autofluorescence in immunolabeling experiments. Cells in the cardiac jelly that showed rounded, spindle-shaped migratory morphology and the absence of a flattened endothelial morphology were defined as mesenchymal cells.

2.6. AMIRA 3D reconstruction of protein distributions in the OFT cushion

AMIRA (Visage Imaging, Andover, MA) was used to generate three-dimensional (3D) images of Fbln1 (E9.5 and E10.5) and TGFβ2 (E9.5) protein distribution. Quantification of TGFβ2 positive tissue was performed by summing the positive pixels (i.e., Cy5-labeled donkey anti-mouse detection of anti-TGFβ2 IgG) in a series of voxels in a stack from each OFT tissue (i.e., 5 μm sections of OFT cushions for anti-TGFβ2). Immunostaining conditions for wild type and Fbln1 null sections were performed under identical conditions; images were acquired by confocal microscopy using the same laser and gain settings.

2.7. Benzidine staining

Paraffin sections of OFT regions from wild type and Fbln1 null embryos were deparaffinized in xylenes and rehydrated through an ethanol gradient. Sections were then washed in PBS for 5 min and stained with 3′3-diaminobenzidine reagent (Sigma-Aldrich) for 1 h at RT in accordance with the manufacturer's recommendations (Lu et al., 2008). Slides were subsequently counterstained with eosin. Hemoglobin-containing cells (e.g., erythrocytes) were detected based on their brown staining.

2.8. Generation of Fbln1-depleted serum

An anti-Fbln1 IgG column was generated by coupling the monoclonal antibody 3A11 to Sepharose (Tran et al., 1997). Fbln1 was depleted from Fetal Bovine Serum (FBS) by passing the serum over the monoclonal anti-Fbln1 3A11 IgG Sepharose column six times. Depletion of Fbln1 protein was verified by ELISA or immunoblotting.

2.9. OFT cushion explant EMT assay

OFT regions were dissected out of wild type and Fbln1 null hearts from E10.5 embryos (Bernanke and Markwald, 1982; Sugi et al., 2004). The proximal OFT regions (Wu et al., 2011) were cut longitudinally and the endocardial side placed on a collagen gel (i.e., rat-tail type I collagen, 1 mg/ml,) equilibrated with OptiMEM (Invitrogen) medium supplemented with Fbln1-depleted fetal bovine serum (1% heat-inactivated), 1% ITS and 1% penicillin/streptomycin. Following 2 h of incubation at 37 °C, additional medium was added and collagen gels were incubated for 48 h. EMT was assessed at 48 h using Hoffman optics on an inverted Leica microscope to count the number of cells that migrated from the explants into the collagen gels.

Author Manuscript Author Manuscript Author Manuscript Author Manuscript

2.10. Statistical analysis

Fisher's exact test and Student's t-test (unpaired, two tailed variants) were used to determine the statistical significance of experimental results using Prism version 6.01 software (GraphPad, La Jolla, CA). Differences were considered significant at $p < 0.05$.

3. Results

3.1. Fbln1 is expressed by the proximal and distal OFT cushions at E9.5 and E10.5

Immunolabeling of E9.5 wild type OFT sections (Fig. 1A and B) showed that Fbln1 was detected in the ECM adjacent to the endothelium of the proximal and distal OFT cushions (Fig. 1A and B). Similarly, at E10.5 Fbln1 was detected in the ECM adjacent to the endothelium and also around the EMT-derived mesenchymal cells (Fig. 1D and E) of the OFT.

To further evaluate the spatiotemporal pattern of Fbln1, we generated three-dimensional (3D) reconstructions of E9.5 and E10.5 OFT cushion regions using AMIRA (Fig. 1C and F). In both reconstructions, Hoechst-stained cells (blue) marked the endocardial cells and the EMT-derived mesenchymal cells adjacent to the OFT lumen. Fbln1 expression (red) was evident in cellular cushion regions that are adjacent to the lumen (Fig. 1C and F). Analysis of the 3D renderings showed that Fbln1 was deposited in the ECM of the distal and proximal OFT regions at both E9.5 and E10.5.

3.2. Fbln1 deficiency results in hypercellular OFT cushions at E9.5

EMT initiates in the mouse OFT at approximately E10.5 (Garside et al., 2012). As expected, examination of wild type embryos showed that very few cells were present in the OFT cushions at E9.5 (Fig. 2A). By contrast, analysis of Fbln1-deficient embryos revealed an abundance of cells present in the proximal OFT cushions at E9.5 (Fig. 2B). Many of these cells had the characteristics of mesenchyme, i.e., a rounded, spindle-shaped migratory morphology. Interestingly, other cells present in the cushions were distinctly round, stained intensely red by H&E (and blue by Giemsa, Supplemental Fig. S1) and generally appeared to be erythrocytes (Fig. 2D). Benzidine staining was performed to determine whether these cells were positive for hemoglobin. As shown in Fig. 2E, cells inside the OFT lumen of wild type embryos stained positively for hemoglobin, as would be expected for erythrocytes circulating at this stage. Analysis of the Fbln-1 null OFT samples revealed that the presumptive erythrocytes present within the cushions also stained positively for hemoglobin (Fig. 2F). Notably, the erythrocytes in the lumen and the cushions were nucleated, which is characteristic of primitive erythrocytes that are present at this developmental stage. Thus, in addition to the increase in mesenchymal cells, there was accumulation of at least one type of blood cell in the proximal OFT cushions in Fbln1 nulls at E9.5.

Quantitative analysis of cell types present in the proximal OFT at E9.5 showed that there was no difference in the number of endothelial cells between wild type and Fbln1 deficient embryos (Table 1). However, as shown in Fig. 2G, the total number of mesenchymal cells was increased in the proximal OFT of Fbln1 nulls compared to wild types (354% increase, $p = 0.0002$). Additionally, quantitative analysis of erythrocyte numbers revealed that there was

Author Manuscript Author Manuscript Author Manuscript Author Manuscript

a complete absence of these cells in the cushion of wild type samples while there was a mean of approximately 0.48 blood cells/mm (Garside et al., 2012) in Fbln1 null proximal OFT cushions at this stage (Fig. 2H; Table 1) (n = 4 for each genotype).

The increase in mesenchymal cell number suggested the possibility that cell proliferation rates were increased in Fbln1 null embryos. PHH3 immunolabeling was performed to quantify cell proliferation rates in proximal OFT of E9.5 wild type and Fbln1 null embryos. However, analysis of PHH3 positive cells detected no apparent difference in proliferation of mesenchymal and endothelial cells between wild type and Fbln1 null E9.5 OFT cushions (Table 1).

To visualize and compare endothelial, mesenchymal, and erythrocyte content in the entire E9.5 proximal OFT cushion, AMIRA 3D reconstructions were generated for wild type and Fbln1 null embryos. Reconstructions of the wild type cushion revealed the endothelial cell-containing region (*purple*), but also showed the near absence of mesenchymal cells (*blue*) and the complete absence of blood cells (*red*) (Fig. 2I). These patterns were starkly contrasted in the Fbln1 null reconstructions (Fig. 2J), which showed abundant mesenchymal and erythrocyte-containing regions throughout the length of the proximal OFT. Taken together, these results indicate that Fbln1 normally limits EMT in the proximal OFT at E9.5 and prevents accumulation of blood cells.

3.3. Fbln1 deficiency results in hypercellular OFT cushions at E10.5

Analysis of OFT cushions at E10.5 again revealed differences in cellular content between wild type and Fbln1 null embryos. Mesenchymal cell numbers in the proximal OFT cushions of Fbln1 nulls were increased by approximately 50% compared to wild type ($p = 0.06$; $n = 5$) (Fig. 3A; Table 2). By contrast, distal OFT cushions at this stage showed no significant difference in the number of mesenchymal cells between Fbln1 null and wild type samples ($p = 0.87$; $n = 5$) (Fig. 3B). Additionally, there was no difference in levels of apoptosis ($p = 0.53$; $n = 5$) or proliferation ($p = 0.49$; $n = 5$) in the distal OFT at this stage (Fig. 3C–E). Erythrocytes were detected in both the proximal (Table 2) and distal OFT cushions of Fbln1 nulls at E10.5 while none were detected in either cushions in wild types (Supplemental Fig. S3).The number of erythrocytes in the proximal OFT cushions of Fbln1 nulls was notably higher than in the distal cushions.Taken together, these findings indicate that Fbln1 limits EMT in the proximal OFT at E10.5 and prevents blood cells from accumulating in both the proximal and distal cushions.

3.4. Fbln1 deficiency results in increased EMT in OFT cushion explant cultures at E10.5

To assess the effect of Fbln1 deficiency on OFT EMT, explant culture assays were performed on OFT samples taken from E10.5 wild type and Fbln1 null embryos. Micrographs of explants cultured for 48 h revealed an apparent increase in cell outgrowth in the Fbln1 null explant compared to wild type (Fig. 4A and B). Quantitative analysis confirmed that Fbln1 null OFT cushion explants showed a 58% increase in outgrowth cells compared to wild type samples ($p = 0.005$; $n = 4$) (Fig. 4). These findings support the conclusion that Fbln1 normally suppresses EMT in the proximal OFT.

Author Manuscript Author Manuscript Author Manuscript Author Manuscript

3.5. Fbln1 deficiency results in increased TGFβ2 and Snail1 levels in OFT cushions at E9.5

To investigate potential linkages between Fbln1 and the increased EMT observed in Fbln1 null embryos, we examined the expression of TGFβ2 and its transcriptional target Snail1, which together represent an established positive regulator of EMT (Niessen et al., 2008). Immunolabeling of E9.5 OFT cushions showed that there was a 58% increase in TGFβ2 protein in the proximal OFT of Fbln1 nulls compared to wild type ($p = 0.01$, $n = 3$) (Fig. 5A–C). The TGFβ2-induced gene, Snail1, also showed a 27% increase in immunoreactivity in the proximal OFT of Fbln1 null cushions at E9.5 ($p = 0.0003$, $n = 4$) (Fig. 5D–F). These findings suggest that Fbln1 normally suppresses proximal OFT EMT through a mechanism(s) that may involve negative feedback on the TGF β2/Snail1 pathway, thereby preventing endocardial cushion hypercellularity.

4. Discussion

The mouse heart at E8.5-E9.0 is a simple linear tube that consists of an endothelium surrounded by ECM and several layers of myocardium. The primitive heart tube undergoes rightward rotation to form a single atrium and ventricle along with two areas of constriction: 1) the atrioventricular canal (AVC) located between the atrium and the ventricle, and 2) the OFT located between the ventricle and the aortic sac. In response to myocardial-derived Bmp, these two regions, AVC and OFT, express hyaluronan resulting in localized swellings of ECM to form the primitive acelluar AV and OFT endocardial cushions (Bai et al., 2013; Ma et al., 2005; Shirai et al., 2009; Sugi et al., 2004). Development of OFT cushions into the semilunar valves requires that the acellular ECM be populated by mesenchymal cells derived from several sources, including EMT, neural crest and secondary heart field (Combs and Yutzey, 2009). Collectively the OFT cushions are comprised of distal cushions, proximal cushions and a pair of intercalated cushions, and give rise to the transient septum, arterial walls and semilunar valve leaflets. In the post-natal heart, mesenchymal cells originating from NCC are present in the arterial walls and in the semilunar valve leaflets (Jiang et al., 2000; Phillips et al., 2013) while cells originating from proximal cushion EMT reside almost exclusively in the fully formed semilunar valve cusps (de Lange et al., 2004; Phillips et al., 2013). There is some indication that semilunar valve leaflets derived from the intercalated cushions, that form later in development, have reduced numbers of neural crest derived cells (Phillips et al., 2013). The contribution of neural crest- and EMT-derived cells to the post-natal semilunar valves has not been studied extensively.

Although several ECM proteins are known to influence EMT, the majority of these proteins promote mesenchymal cell invasion of the endocardial cushions (Camenisch et al., 2000; Garside et al., 2012; Mjaatvedt et al., 1998; Patra et al., 2011). Relatively few proteins are known to negatively regulate OFT EMT and cushion invasion (Dor et al., 2001). Here, our results demonstrate that the ECM protein Fbln1 is a negative regulator of cardiac OFT EMT. First, Fbln1 deficiency resulted in increased EMT that led to a hypercellular proximal OFT cushion phenotype at E9.5–E10.5. Second, cushion explant cultures prepared from E10.5 proximal OFTs showed that Fbln1 null samples had a 58% increase in the number of migratory cells. Together these findings indicate that Fbln1 normally suppresses cardiac OFT EMT at E9.5–E10.5. Furthermore, these findings are consistent with prior studies

Author Manuscript Author Manuscript Author Manuscript Author Manuscript

showing that exogenous Fbln1 inhibited invasion of endocardial cushion mesenchymal cells migrating from cultured embryonic heart explants (Twal et al., 2001).

Our results also indicate that Fbln1 is a suppressor of TGFβ2 and Snail1 production during proximal OFT development. We speculate that the elevated TGFβ2 observed in Fbln1 nulls causes an increase in Snail1 expression and a subsequent increase in EMT in the proximal OFT. This would be consistent with previous studies showing that TGFβ2 directly induces transcription of Snail1, which is implicated in the initiation of EMT (Niessen et al., 2008; Timmerman et al., 2004), and that increased TGFβ2 expression causes increased EMT (Shirai et al., 2009) and a hypercellular cushion phenotype (Sakabe et al., 2012; Shirai et al., 2009). Furthermore, the induction of Snail1 expression by TGFβ2 treatment has been shown to rescue EMT defects in the developing heart (Niessen et al., 2008).

While the underlying mechanism by which Fbln1 represses the TGFβ2/Snail1 pathway remains to be studied, one possible mechanism would be that Fbln1 influences the release of TGFβ2 from the ECM. The secreted ECM protein Emilin-1 has been shown to bind to the TGFβ precursor, proTGFβ, and prevent its maturation and bioavailability (Zacchigna et al., 2006). Taking into account that TGFβ2 levels are increased in the absence of Fbln1, it is possible that Fbln1 normally acts as a negative regulator of TGFβ2 by directly binding to either the large latent complex or the small latent complex, making it less accessible to proteolytic cleavage by matrix metalloproteinases (MMPs), thereby limiting its release from the ECM and reducing bioavailability of TGFβ2 during OFT cushion morphogenesis.

Findings from this study also revealed that loss of Fbln1 resulted in the accumulation of cells in the proximal OFT cushions at E9.5 and E10.5 that were judged to be erythrocytes. This conclusion was based on round morphology of the cells, intense staining with Giemsa, autofluorescence in immunological staining, and expression of hemoglobin. Hematopoiesis begins in the mouse in the yolk sac at approximately E7, and primitive erythrocytes enter the blood stream when circulation is established at approximately E8.5 (Palis et al., 1999). At the stages examined in this study, erythrocytes constitute the majority of the circulating blood cell population (Hirschi, 2012; Palis et al., 1999; Silver and Palis, 1997).

The mechanism by which erythrocytes accumulate in the OFT cushions has not been established. One possibility is that circulating cells enter the cushions from the OFT lumen. During EMT, the endocardium is permeable as the endocardial cells lose their polarity and start migrating into the cushions (Garside et al., 2012; Lim and Thiery, 2012). The loss of Fbln1, and the enhanced EMT that follows, may further destabilize the proximal OFT endothelial barrier at E9.5, allowing entry of circulating cells into the proximal OFT cushions. Such an explanation would account for the elevated number of erythrocytes in the proximal cushions, where EMT occurs, compared to the distal cushions, where the mesenchyme is populated primarily by migrating neural crest cells (Wu et al., 2011). However, the fact that erythrocytes were also present in the distal OFT cushions would suggest that Fbln1 normally provides stabilization of the OFT endocardium irrespective of EMT. Previous studies have shown that mice deficient in Fbln1 display defects in the endothelial layer of some blood vessels that is characterized by dilation and rupture (Kostka et al., 2001). Those findings support the possibility that endocardial barrier is compromised

Author Manuscript Author Manuscript Author Manuscript Author Manuscript

by the loss of Fbln1, and that erythrocytes in circulating blood enter the cushions due to endocardial barrier disruption.

A second possibility is that in the absence of Fbln1, erythrocytes originate *in situ* in the OFT cushions. OFT endocardium (Nakano et al., 2013; Van Handel et al., 2012) has been shown to have hemogenic potential that begins at around E9.5. It is possible that Fbln1 supports this specification in a way that maintains production of hematopoietic cells on the luminal side of the endocardium. Thus, in the absence of Fbln1, the hemogenic OFT endocardium may generate erythrocytes on the inner (i.e, cardiac jelly) side of the endocardium. Studies of the effect of T cell acute lymphocytic leukemia 1 deficiency (Scl/tal1) in cardiac cushions have shown that such a misspecification of endocardium can occur (Nakano et al., 2013).

Here we have shown that the ECM protein Fbln1 is important for mouse OFT morphogenesis. Fbln1 is present in proximal and distal OFT cushions, and our results indicate that Fbln1 normally suppresses EMT in the proximal OFT cushion and prevents hypercellularity, including the accumulation of erythrocytes. The loss of Fbln1 was linked to the upregulation of both TGFβ2 and Snail1, both established stimulators of EMT. Future experiments are expected to elucidate how Fbln1 influences the TGFβ2/Snail1 pathway and how Fbln1 stabilizes the structure and/or specification of the OFT endocardium.

Supplementary Material

Refer to Web version on PubMed Central for supplementary material.

Acknowledgments

We thank Marie Lockhart for helping with AMIRA 3D reconstruction of Fbln1 expression.

Source of funding

This work was supported by NIH grant HL95067 (WSA). CBK was supported by American Heart Association grant 10SDG2610168. YS was supported by AHA Grant-in-Aid 10GRNT3900044 and Lawrence J. and Florence A. DeGeorge Charitable Trust. JLB was supported by NIH grants P30GM103342 and P20GM103499. This study used the services of the Morphology, Imaging and Instrumentation Core, which is supported by NIH-NIGMS P30GM103342 to the South Carolina COBRE for Developmentally Based Cardiovascular Diseases.

Abbreviations

OFT	outflow tract
AV	atrioventricular
EC	endocardial cushions
EMT	endothelial to mesenchymal transition
SMA	smooth muscle actin
TGF	transforming growth factor
NCC	neural crest cells

Author Manuscript Author Manuscript Author Manuscript Author Manuscript

REFERENCES

Anderson RH, Webb S, Brown NA, Lamers W, Moorman A. Development of the heart: (3) formation of the ventricular outflow tracts, arterial valves, and intrapericardial arterial trunks. Heart. 2003; 89(9):1110–1118. [PubMed: 12923046]

Argraves WS, Tran H, Burgess WH, Dickerson K. Fibulin is an extracellular matrix and plasma glycoprotein with repeated domain structure. J. Cell Biol. 1990; 111(6 Pt 2):3155–3164. [PubMed: 2269669]

Bai Y, Wang J, Morikawa Y, Bonilla-Claudio M, Klysik E, Martin JF. Bmp signaling represses Vegfa to promote outflow tract cushion development. Development. 2013; 140(16):3395–3402. [PubMed: 23863481]

Barnett JV, Desgrosellier JS. Early events in valvulogenesis: a signaling perspective. Birth Defects Res. C Embryo Today. 2003; 69(1):58–72. [PubMed: 12768658]

Bernanke DH, Markwald RR. Migratory behavior of cardiac cushion tissue cells in a collagen-lattice culture system. Dev. Biol. 1982; 91(2):235–245. [PubMed: 7095266]

Bouchey D, Argraves WS, Little CD. Fibulin-1, vitronectin, and fibronectin expression during avian cardiac valve and septa development. Anat. Rec. 1996; 244(4):540–551. [PubMed: 8694289]

Butcher JT, Markwald RR. Valvulogenesis: the moving target. Philos. Trans. R. Soc. Lond. B. Biol Sci. 2007; 362(1484):1489–1503. [PubMed: 17569640]

Camenisch TD, Spicer AP, Brehm-Gibson T, Biesterfeldt J, Augustine ML, Calabro A Jr. et al. Disruption of hyaluronan synthase-2 abrogates normal cardiac morphogenesis and hyaluronan-mediated transformation of epithelium to mesenchyme. J. Clin. Invest. 2000; 106(3):349–360. [PubMed: 10930438]

Camenisch TD, Schroeder JA, Bradley J, Klewer SE, McDonald JA. Heart-valve mesenchyme formation is dependent on hyaluronan-augmented activation of ErbB2-ErbB3 receptors. Nat. Med. 2002; 8(8):850–855. [PubMed: 12134143]

Combs MD, Yutzey KE. Heart valve development: regulatory networks in development and disease. Circ. Res. 2009; 105(5):408–421. [PubMed: 19713546]

Cooley MA, Kern CB, Fresco VM, Wessels A, Thompson RP, McQuinn TC, et al. Fibulin-1 is required for morphogenesis of neural crest-derived structures. Dev. Biol. 2008; 319(2):336–345. [PubMed: 18538758]

de Lange FJ, Moorman AF, Anderson RH, Manner J, Soufan AT, de Gier-de Vries C, et al. Lineage and morphogenetic analysis of the cardiac valves. Circ. Res. 2004; 95(6):645–654. [PubMed: 15297379]

Dor Y, Camenisch TD, Itin A, Fishman GI, McDonald JA, Carmeliet P, et al. A novel role for VEGF in endocardial cushion formation and its potential contribution to congenital heart defects. Development. 2001; 128(9):1531–1538. [PubMed: 11290292]

Garside VC, Chang AC, Karsan A, Hoodless PA. Coordinating Notch, BMP, and TGF-beta signaling during heart valve development. Cell. Mol. Life Sci. 2012; 70(16):2899–2917. [PubMed: 23161060]

Hirschi KK. Hemogenic endothelium during development and beyond. Blood. 2012; 119(21):4823–4827. [PubMed: 22415753]

Jiang X, Rowitch DH, Soriano P, McMahon AP, Sucov HM. Fate of the mammalian cardiac neural crest. Development. 2000; 127(8):1607–1616. [PubMed: 10725237]

Kostka G, Giltay R, Bloch W, Addicks K, Timpl R, Fassler R, et al. Perinatal lethality and endothelial cell abnormalities in several vessel compartments of fibulin-1-deficient mice. Mol. Cell. Biol. 2001; 21(20):7025–7034. [PubMed: 11564885]

Lim J, Thiery JP. Epithelial-mesenchymal transitions: insights from development. Development. 2012; 139(19):3471–3486. [PubMed: 22949611]

Lu SJ, Feng Q, Park JS, Vida L, Lee BS, Strausbauch M, et al. Biologic properties and enucleation of red blood cells from human embryonic stem cells. Blood. 2008; 112(12):4475–4484. [PubMed: 18713948]

Author Manuscript Author Manuscript Author Manuscript Author Manuscript

Ma L, Lu MF, Schwartz RJ, Martin JF. Bmp2 is essential for cardiac cushion epithelial-mesenchymal transition and myocardial patterning. Development. 2005; 132(24):5601–5611. [PubMed: 16314491]

Mjaatvedt CH, Yamamura H, Capehart AA, Turner D, Markwald RR. The Cspg2 gene, disrupted in the hdf mutant, is required for right cardiac chamber and endocardial cushion formation. Dev. Biol. 1998; 202(1):56–66. [PubMed: 9758703]

Nakano H, Liu X, Arshi A, Nakashima Y, van Handel B, Sasidharan R, et al. Haemogenic endocardium contributes to transient definitive haematopoiesis. Nat. Commun. 2013; 4:1564. [PubMed: 23463007]

Niessen K, Fu Y, Chang L, Hoodless PA, McFadden D, Karsan A. Slug is a direct Notch target required for initiation of cardiac cushion cellularization. J. Cell Biol. 2008; 182(2):315–325. [PubMed: 18663143]

Palis J, Robertson S, Kennedy M, Wall C, Keller G. Development of erythroid and myeloid progenitors in the yolk sac and embryo proper of the mouse. Development. 1999; 126(22):5073–5084. [PubMed: 10529424]

Patra C, Diehl F, Ferrazzi F, van Amerongen MJ, Novoyatleva T, Schaefer L, et al. Nephronectin regulates atrioventricular canal differentiation via Bmp4-Has2 signaling in zebrafish. Development. 2011; 138(20):4499–4509. [PubMed: 21937601]

Phillips HM, Mahendran P, Singh E, Anderson RH, Chaudhry B, Henderson DJ. Neural crest cells are required for correct positioning of the developing outflow cushions and pattern the arterial valve leaflets. Cardiovasc. Res. 2013; 99(3):452–460. [PubMed: 23723064]

Sakabe M, Kokubo H, Nakajima Y, Saga Y. Ectopic retinoic acid signaling affects outflow tract cushion development through suppression of the myocardial Tbx2-Tgfbeta2 pathway. Development. 2012; 139(2):385–395. [PubMed: 22186728]

Shirai M, Imanaka-Yoshida K, Schneider MD, Schwartz RJ, Morisaki T. T-box 2, a mediator of Bmp-Smad signaling, induced hyaluronan synthase 2 and Tgfbeta2 expression and endocardial cushion formation. Proc. Natl. Acad. Sci. U.S.A. 2009; 106(44):18604–18609. [PubMed: 19846762]

Silver L, Palis J. Initiation of murine embryonic erythropoiesis: a spatial analysis. Blood. 1997; 89(4): 1154–1164. [PubMed: 9028937]

Sizarov A, Lamers WH, Mohun TJ, Brown NA, Anderson RH, Moorman AF. Three-dimensional and molecular analysis of the arterial pole of the developing human heart. J. Anat. 2012; 220(4):336–349. [PubMed: 22296102]

Sugi Y, Yamamura H, Okagawa H, Markwald RR. Bone morphogenetic protein-2 can mediate myocardial regulation of atrioventricular cushion mesenchymal cell formation in mice. Dev. Biol. 2004; 269(2):505–518. [PubMed: 15110716]

Timmerman LA, Grego-Bessa J, Raya A, Bertran E, Perez-Pomares JM, Diez J, et al. Notch promotes epithelialmesenchymal transition during cardiac development and oncogenic transformation. Genes Dev. 2004; 18(1):99–115. [PubMed: 14701881]

Tran H, VanDusen WJ, Argraves WS. The self-association and fibronectin-binding sites of fibulin-1 map to calcium-binding epidermal growth factor-like domains. J. Biol. Chem. 1997; 272(36): 22600–22606. [PubMed: 9278415]

Twal WO, Czirok A, Hegedus B, Knaak C, Chintalapudi MR, Okagawa H, et al. Fibulin-1 suppression of fibronectin-regulated cell adhesion and motility. J. Cell Sci. 2001; 114(Pt 24):4587–4598. [PubMed: 11792823]

Van Handel B, Montel-Hagen A, Sasidharan R, Nakano H, Ferrari R, Boogerd CJ, et al. Scl represses cardiomyogenesis in prospective hemogenic endothelium and endocardium. Cell. 2012; 150(3): 590–605. [PubMed: 22863011]

Waldo K, Miyagawa-Tomita S, Kumiski D, Kirby ML. Cardiac neural crest cells provide new insight into septation of the cardiac outflow tract: aortic sac to ventricular septal closure. Dev. Biol. 1998; 196(2):129–144. [PubMed: 9576827]

Wu B, Wang Y, Lui W, Langworthy M, Tompkins KL, Hatzopoulos AK, et al. Nfatc1 coordinates valve endocardial cell lineage development required for heart valve formation. Circ. Res. 2011; 109(2):183–192. [PubMed: 21597012]

Author Manuscript Author Manuscript Author Manuscript Author Manuscript

Zacchigna L, Vecchione C, Notte A, Cordenonsi M, Dupont S, Maretto S, et al. Emilin1 links TGF-beta maturation to blood pressure homeostasis. Cell. 2006; 124(5):929–942. [PubMed: 16530041]

Author Manuscript Author Manuscript Author Manuscript Author Manuscript

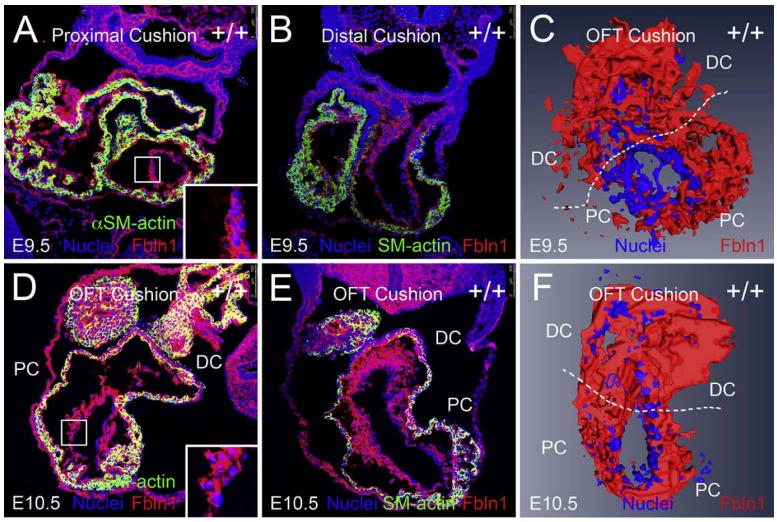

Fig. 1.

Fibulin-1 is present in the proximal and distal OFT cushions at E9.5 and E10.5. (A and B) show cryosections (10 μm) of wild type E9.5 OFT cushions. (A) shows E9.5 proximal cushions and (B) shows E9.5 distal cushions immunolabeled using anti-Fbln1 (*red*) and anti-αSMA (green). Nuclei were stained using Hoechst (*blue*). (D and E) show cryosections (10 μm) of wild type E10.5 OFT cushions. (D) shows E10.5 proximal and (E) shows E10.5 distal cushions immunolabeled using anti-Fbln1 (*red*) and anti-αSMA (*green*). Nuclei were stained using Hoechst (*blue*). Inset boxes in A and D show portions of the proximal OFT at higher magnification. Lumen region in insets is to the right; Fbln1 (*red*) is seen on the inner surface and in close association with the endocardium (*blue* nuclei). Shown in A–B and D–E are representative images of OFT cushions from 2 different wild type E9.5-E10.5 embryos. PC, proximal cushions; DC, distal cushions. All sections are transverse. (C and F) AMIRA-based 3D reconstructions of OFT, endothelial and EMT-derived mesenchymal cells (both Hoechst labeled, *blue*) and adjacent Fbln1 (*red*) in wild type E9.5-E10.5 proximal and distal OFT. 3D reconstruction regions are limited to the EMT-derived sections of E9.5-E10.5 proximal and distal OFT cushions. PC, proximal OFT cushions; DC, distal OFT cushions.

Author Manuscript Author Manuscript Author Manuscript Author Manuscript

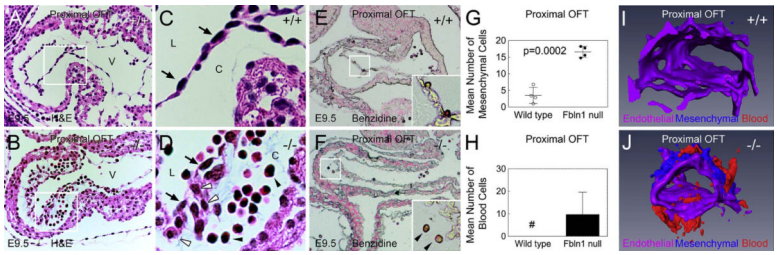

Fig. 2.

Fibulin-1 deficient embryos display hypercellular OFT cushions and blood cell accumulation in OFT cushions at E9.5. (A and B) H&E stained E9.5 sections of proximal OFT cushions from wild type and Fbln1 null embryos, respectively. Note the abundant cells present in the cushion of the Fbln1 null section compared to the wild type. (C) shows a higher magnification of boxed region in (A). Note endothelial cells (black arrows) lining the OFT lumen (L) and the absence of mesenchymal cells in the wild type cushion (C). (D) shows higher magnification view of boxed region in (B) showing endothelial cells (black arrows) lining the lumen of the OFT of a Fbln1 null. Note the presence of mesenchymal cells (white arrowheads) and blood cells (black arrowheads) in the proximal cardiac jelly of the Fbln1 null. (E and F) show E9.5 wild type and Fbln1 null proximal OFT cushions stained with Benzidine (brown) to label hemoglobin-producing cells. Sections were counterstained briefly with Eosin. Inset in (E) shows higher magnification of hemoglobin positive cells located normally within the lumen of wild type proximal OFT cushions. Inset in (F) shows higher magnification of hemoglobin positive cells in the cardiac jelly region of Fbln1 null proximal OFT cushions. All sections are sagittal. (G) and (H) show quantification of mesenchymal and blood cells, respectively, present in wild type and Fbln1 null proximal OFT cushions. (G) Fbln1 nulls show a 354% increase ($p = 0.0002$) in mesenchymal cells present in the cushions. Cell counts were obtained from 54 sections from four wild type embryos and 54 sections from four Fbln1 null embryos. Pound (#) in (H) indicates that no blood cells were detected in wild type proximal cushions at E9.5. (I) and (J) show AMIRA 3D reconstructions of wild type and Fbln1 null proximal OFT cushions at E9.5. (I) 3D reconstruction of wild type shows endocardial cell content but little mesenchymal cell content (*blue*) and no blood cell content in the cushion. (J) 3D reconstruction of Fbln1 null shows an increase in mesenchymal cell content (*blue*) and the presence of blood cells (*red*) in the proximal cushions. C, proximal OFT cushions; L, lumen of OFT.

Author Manuscript Author Manuscript Author Manuscript Author Manuscript

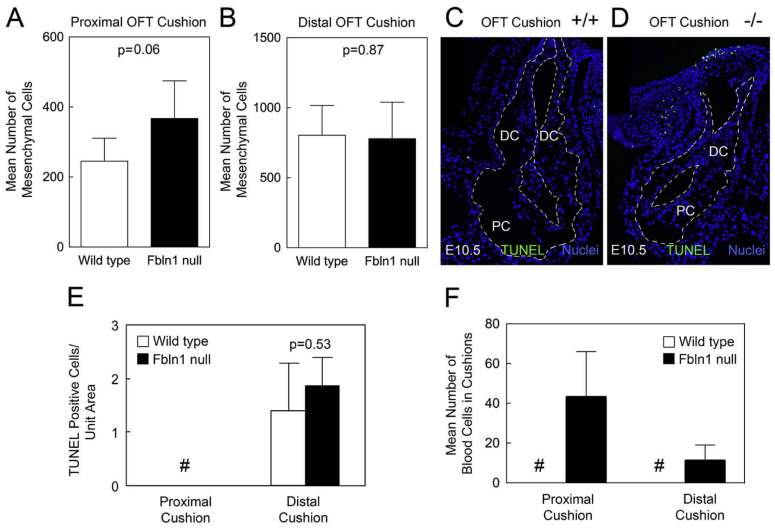

Fig. 3.

Fibulin-1 deficient E10.5 proximal OFT cushions display increased mesenchymal cells, blood cell infiltration and no difference in apoptosis. (A) shows that Fbln1 null E10.5 proximal OFT cushions have an increase in mesenchymal cells compared to wild type proximal cushions ($p = 0.06$); graphs were based on cell counts of 37 sections from 5 wild type embryos and 37 sections from 5 Fbln1 null embryos. (B) shows no difference in the average number of mesenchymal cells in E10.5 distal OFT cushions of wild type and Fbln1 null embryos ($p = 0.87$). Graphs were based on cell counts of 37 sections from 5 wild type embryos and 37 sections from 5 Fbln1 null embryos. (C and D) micrographs showing fluorescence staining of TUNEL positive cells in E10.5 wild type and Fbln1 null, respectively, proximal and distal OFT cushions. Nuclei were stained using Hoechst (*blue*). All sections are sagittal. (E) quantification of TUNEL positive cell data for E10.5 wild type and Fbln1 null proximal and distal OFT cushions. Pound (#) indicates that TUNEL positive cells were not detected in the proximal OFT. Although the mean number of TUNEL positive cells was slightly greater in the Fbln1 null distal OFT relative to wild type, differences were not significant ($p = 0.53$). (F) shows a graph depicting the average number of blood cells in E10.5 proximal OFT cushions. Blood cell counts were performed on 37 sections from 5 wild type embryos and 37 sections from 5 Fbln1 null embryos. Results showed that in Fbln1 nulls the numbers of blood cells were increased as compared to wild type. Pound (#) indicates that blood cells were not detected in wild type proximal or distal OFT cushions. PC, proximal OFT cushions; DC, distal OFT cushions.

Author Manuscript Author Manuscript Author Manuscript Author Manuscript

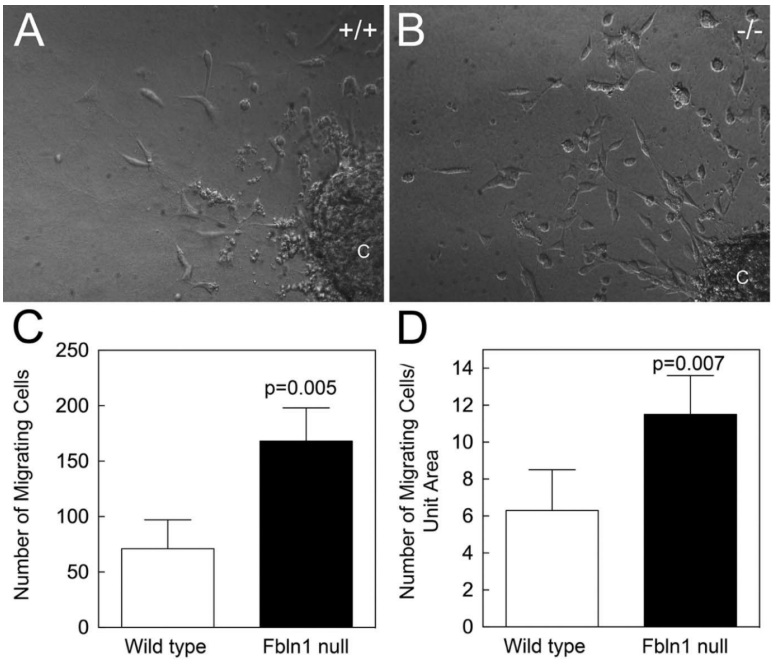

Fig. 4.

Fibulin-1 deficient E10.5 proximal OFT cushion explants display increased EMT. (A and B), proximal OFT cushion explants from E10.5 wild type and Fbln1 null embryos were cultured for 48 h on collagen gels. (C) Graph depicting the number of wild type and Fbln1 null cells that migrated from the explants into the collagen gel. Fbln1 null explants showed a 58% increase in cell number ($p = 0.005$; based on cell counts of 4 wild type and 4 Fbln1 null explants). (D) Graph depicting the number of wild type and Fbln1 null migrating cells per unit area, again illustrating that Fbln1 nulls showed a significant increase in cell outgrowth ($p = 0.007$). C, proximal OFT cushion explant.

Author Manuscript Author Manuscript Author Manuscript Author Manuscript

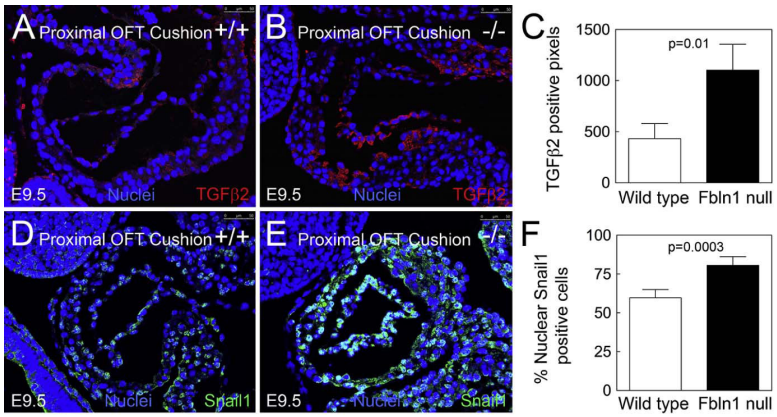

Fig. 5.

Fibulin-1 deficient E9.5 proximal OFT cushions display increases in TGFβ2 and Snail1 protein levels. (A) and (B) show immunolabeling of TGFβ2 (*red*) in proximal OFT cushions from E9.5 wild type (A) or Fbln1 null (B) embryos. (C) shows a graph depicting the greater number of TGFβ2 positive pixels in the E9.5 proximal OFT cushions of Fbln1 null embryos ($p = 0.01$) compared to wild types. Data were obtained from the analysis of 3 sections from 3 wild type embryos and 3 sections from 3 Fbln1 null embryos. (D and E) show immunolabeling of Snail1 (*green*) in proximal OFT cushions from E9.5 wild type (D) or Fbln1 null (E) embryos. All sections are sagittal. (F) A graph depicting the percentage of Snail1 positive nuclei in the E9.5 proximal OFT cushions of wild type and Fbln1 null embryos as a function of total number of cells ($p = 0.0003$). Data were obtained from the analysis of 19 sections from four wild type embryos and 19 sections from 4 Fbln1 null embryos. Scale bar 50 μm.

Author Manuscript

Author Manuscript

Author Manuscript

Author Manuscript

Table 1

Analysis of E9.5 wild type and Fbln1 null proximal outflow tract cushions.

Metric	Wild type[e]	Fibulin-1 null[f]	% Change[g]	P value[h]
Endothelial cell numbers (mean) proximal OFT[a]	26 ± 4.1	32 ± 5.1	23.1	0.11
Mesenchymal cell numbers (mean) proximal OFT[a]	3.5 ± 2.4	15.9 ± 2.24	354.3	0.0002
Total number of blood cells proximal OFT[a]	0	9.18 ± 10.74	NA	0.13
Total number of cells (endothelial, mesenchymal, blood cells)[a]	29.5 ± 6.2	57 ± 8.7	93.2	0.002
Ratio of mesenchymal:endothelial cells[a]	0.12 ± 0.07	0.49 ± 0.07	308.3	0.0004
Proximal OFT cushion area (mm^2)[b]	23 ± 5.6	18.4 ± 1.14	−21.4	0.13
Endothelial cells/mm^2[c]	1.15 ± 0.35	1.73 ± 0.23	50.4	0.03
Mesenchymal cells/mm^2[c]	0.16 ± 0.14	0.86 ± 0.15	437	0.028
Blood cells/mm^2[c]	0	0.48 ± 0.56	NA	0.13
Total Cells (endothelial, mesenchymal, blood cells)/mm^2[c]	1.32 ± 0.49	3.09 ± 0.35	134.1	0.001
Percent positive PHH3 cells (endothelial, mesenchymal cells)[d]	10 ± 3	14± 5	40.0	0.29

Mean values ± standard deviation are indicated.NA, calculation not applicable.

a,b,c The data were obtained from analysis of 54 sections from 4 wild type and 54 sections from 4 Fbln1 null embryos.

a,d P value was calculated using Fisher's exact test.

[a]Proximal OFT endothelial, mesenchymal cells and blood cell counts were counted in H&E stained tissue sections of E9.5 wild type and Fbln1 null embryos.

[b]Area (arbitrary units) of the proximal OFT cushion was calculated using Image J software.

[c]Measurements obtained from the mean number of cells in proximal OFT and mean proximal OFT area.

[d]Calculated by counting the number of anti-PHH3 positive cells relative to the total number of nuclei using the Adobe Photoshop Count tool. PHH3 analysis was performed on 15 sections from 2 wild type and 15 sections from 2 Fbln1 null embryos.

[e]n = 4.

[f]n = 4.

[g]Percent change calculated as change in Fbln1 null relative to wild type.

[h]P value was calculated using Student's t-test.

Author Manuscript

Author Manuscript

Author Manuscript

Author Manuscript

Table 2

Analysis of E10.5 wild type and Fbln1 null proximal outflow tract cushions.

Metric	Wild type[e]	Fibulin-1 null[f]	% Change[g]	P value[h]
Endothelial cell numbers (mean) proximal OFT[a]	236 ± 37	278 ± 74	17.8	0.299
Mesenchymal cell numbers (mean) proximal OFT[a]	245 ± 65	367 ± 107	49.8	0.06
Total number of blood cells proximal OFT[a]	0	43 ± 24	NA	0.003
Total number of cells (endothelial, mesenchymal, blood cells)[a]	482 ± 91	688 ± 126	42.7	0.01
Ratio of mesenchymal:endothelial cells[a]	1.04 ± 0.23	1.46 ± 0.83	40.4	0.052
Proximal OFT cushion area (mm^2)[b]	222 ± 56	126 ± 23	−43.3	0.007
Endothelial cells/mm^2[c]	1.09 ± 0.17	2.2 ± 0.44	102.3	0.0008
Mesenchymal cells/mm^2[c]	1.13 ± 0.28	3.1 ± 1.6	174.3	0.024
Blood cells/mm^2[c]	0	0.35 ± 0.18	NA	0.002
Total cells (endothelial, mesenchymal, blood cells)/mm^2[c]	2.22 ± 0.39	5.7 ± 1.77	156.4	0.002
Percent positive PHH3 cells (endothelial, mesenchymal cells)[d]	5.12 ± 2.09	7.2 ± 4.9	40.6	0.409

Mean values ± standard deviation are indicated.NA, calculation not applicable.

a,b,c Data were obtained from analysis of 37 sections from 5 wild type and 37 sections from 5 Fbln1 null embryos.

a,d P value was calculated using Fisher's exact test.

[a]Proximal OFT endothelial, mesenchymal cells and blood cell counts were counted in H&E stained tissue sections of E10.5 wild type and Fbln1 null embryos.

[b]Area (arbitrary units) of the proximal OFT cushion was calculated using Image J software.

[c]Measurements obtained from the mean number of cells in proximal OFT and mean proximal OFT area.

[d]Calculated by counting the number of anti-PHH3 positive cells relative to the total number of nuclei using the Adobe Photoshop Count tool. PHH3 analysis was performed on 5 sections from 5 wild type and 5 sections from 5 Fbln1 null embryos.

[e]n = 5.

[f]n = 5.

[g]Percent change calculated as change in Fbln1 null relative to wild type.

[h]P value was calculated using Student's t-test.